Available online at www.sciencedirect.com
SCIENCE DIRECT
ELSEVIER
Journal of the European Ceramic Society 26 (2006) 1889–1893
ECERS
www.elsevier.com/locate/jeurceramsoc

Comparison of microwave dielectric behavior between $Bi_{1.5}Zn_{0.92}Nb_{1.5}O_{6.92}$ and $Bi_{1.5}ZnNb_{1.5}O_7$

M.-C. Wu [a], S. Kamba [b], V. Bovtun [b], W.-F. Su [a,*]

[a] *Department of Materials Science and Engineering, National Taiwan University, Taipei, Taiwan*
[b] *Department of Dielectrics, Institute of Physics, ASCR, Praha, Czech Republic*

Available online 8 November 2005

Abstract

The microwave dielectric, $Bi_{1.5}ZnNb_{1.5}O_7$ exhibits low-temperature dielectric relaxation. To find the origin of the dielectric relaxation of $Bi_{1.5}ZnNb_{1.5}O_7$, we studied the structure and dielectric behavior of $Bi_{1.5}ZnNb_{1.5}O_7$ in detail. The $Bi_{1.5}ZnNb_{1.5}O_7$ is not composed of a single phase pyrochlore structure. Instead, it consists of unusual structure of $Bi_{1.5}Zn_{0.92}Nb_{1.5}O_{6.92}$ and ZnO. The ZnO is distributed evenly in the grain and at the boundary of the $Bi_{1.5}Zn_{0.92}Nb_{1.5}O_{6.92}$ structure. Many small voids (<1 μm) were observed in the samples due to the loss of volatile Bi during sintering. The $Bi_{1.5}Zn_{0.92}Nb_{1.5}O_{6.92}$ exhibited a broad dielectric relaxation between 100 and 400 K at 1.8 GHz, peaking around 230 K. The Fourier transformation IR spectra predict that dielectric relaxation may occur near room temperature during extremely high frequencies (THz). The substitutional point defects in $Bi_{1.5}Zn_{0.92}Nb_{1.5}O_{6.92}$ provide room for dielectric relaxation at microwave frequencies. The low quality factor $Q \times f$ (∼520 GHz) of $Bi_{1.5}Zn_{0.92}Nb_{1.5}O_{6.92}$ results from both the dielectric relaxation of the material and the voids within its microstructure. The presence of ZnO phase in the $Bi_{1.5}ZnNb_{1.5}O_7$ produces interstitial defects that further enhance the dielectric relaxation with reduced quality factor $Q \times f$ (∼426 GHz).

Keywords: Powders-solid state reaction; Dielectric properties; Microstructure

1. Introduction

The demands for miniaturization in microwave communication technologies require continual discovery and innovation in the development of new materials. Most conventional ceramics have excellent microwave dielectric properties, such as BMT ($BaMg_{1/3}Ta_{2/3}O_3$), BNT ($BaO\text{-}Nd_2O_3\text{-}TiO_2$), etc., and sinterabilities above 1300 °C. Considering the high sintering temperature, Ag–Pd electrode is the only choice for multilayer ceramic components (MLCCs). In the microwave frequency range, the dielectric loss of components is mostly attributed to the electrode. Good conductivity of the electrode is important for MLCCs. Thus, it is desirable to replace the poorly conducting and high-cost Ag–Pd electrode with silver electrodes which have better properties and lower cost. However, since the melting temperature of silver is low (961 °C), a low sintering temperature material is required to cofire with silver.

Recently, $Bi_{1.5}ZnNb_{1.5}O_7$ (BZN) has emerged as a good low-sintering (∼1000 °C) microwave material because it exhibits high dielectric constant and low-temperature coefficient of resonance frequency (τ_f).[1–7] Its sintering temperature can be decreased to 950 °C by adding 3.0 wt% $BaCO_3$–CuO into BZN[8] and even lower to 850 °C by adding 2 mol% V_2O_5 to BZN.[9] However, BZN exhibits low temperature (0–200 K) dielectric relaxation behavior at 1 MHz. Upon heating, the relaxation frequency steeply increases according to the Arrhenius law and appears in microwave range at room temperature.[10,11]

Levin et al.[12] investigated the structure of $Bi_{1.5}ZnNb_{1.5}O_7$ that is composed of an unusual cubic pyrochlore single phase consisting of $Bi_{1.5}Zn_{0.92}Nb_{1.5}O_{6.92}$ and small amounts of ZnO. In order to find the origin of the dielectric relaxation of $Bi_{1.5}ZnNb_{1.5}O_7$, we studied the structures and dielectric behaviors of $Bi_{1.5}ZnNb_{1.5}O_7$ in detail. The results are compared with that of $Bi_{1.5}Zn_{0.92}Nb_{1.5}O_{6.92}$.

2. Experimental

Reagent grade oxide powders with an appropriate molar ratio of Bi_2O_3, ZnO, and Nb_2O_5 (99.9% purity each, Alfa Chemicals,

* Corresponding author. Tel.: +866 2 3366 4078; fax: +866 2 3366 4078.
E-mail address: suwf@ntu.edu.tw (W.-F. Su).

0955-2219/$ – see front matter © 2005 Elsevier Ltd. All rights reserved.
doi:10.1016/j.jeurceramsoc.2005.09.025

USA) were used to prepare BZN samples using the conventional mixed solid method. The samples were calcined at 900 °C for 2 h. The crystalline phases of the calcined BZN powder samples were comparable to those reported in the literature.[9,10]

The BZN powder was characterized by light scattering (Zetasizer 3000HS, Malvern Instruments, UK) for particle size, BET for surface area (Micrometrics, ASAP2000 BET, USA), electronic probe microanalyzer (EPMA, Joel, JXA-8600SX, Japan) for chemical composition, and X-ray diffractometer (XRD, PW 1830, Philips, Nederland) for the crystalline structure. The BZN powder was pressed at 500 kg/cm^2 to form tablets (8 mm diameter) and sintered at 1050 °C for 4 h. The distribution of elements in sintered BZN tablets was observed using an electronic probe microanalyzer. The microstructures of sintered samples were evaluated by scanning electron microscopy (SEM) equipped with wavelength dispersive spectrometer (WDS) (Joel, JSM-T100, Japan).

The dielectric properties of sintered BZN tablets were evaluated by Impedance Analyzer (Hewlett Packard, 4291B, USA) in the frequency range of 1 MHz–1.8 GHz and Network Analyzer (Hewlett Packard, 8722ES, USA) in the microwave frequency region. THz measurement (200–750 GHz) was performed using a custom-made time domain THz spectrometer with femtosecond laser system (Quantronix, Odin). Two identical 1 mm [1 1 0] ZnTe single crystals were used to generate (optical rectification) and detect (electro-optic sampling) the THz pulses. Infrared reflectivity spectra were obtained using a Fourier transform spectrometer (Bruker IFS 113v, Germany) in the frequency range of 20–3300 cm^{-1} (0.6–100 THz).

3. Results and discussion

The physical and chemical properties of $Bi_{1.5}Zn_{0.92}Nb_{1.5}O_{6.92}$ and $Bi_{1.5}ZnNb_{1.5}O_7$ powders prepared by the solid mixing method are summarized in Table 1. They have comparable surface areas and particle size. The content of bismuth in both BZN powders was slightly reduced after calcination at 900 °C for 2 h. This might be due to the volatility of bismuth. Despite this, the stable cubic pyrochlore phase was preserved in both samples as shown in their XRD spectra (Fig. 1). Extra XRD peaks of ZnO are observed in the $Bi_{1.5}ZnNb_{1.5}O_7$ sample as compared to $Bi_{1.5}Zn_{0.92}Nb_{1.5}O_{6.92}$. It corresponds to Levin et al., who have shown that $Bi_{1.5}ZnNb_{1.5}O_7$ is thermodynamically unstable, and $Bi_{1.5}ZnNb_{1.5}O_7$ consists of $Bi_{1.5}Zn_{0.92}Nb_{1.5}O_{6.92}$ and small amount of ZnO.[12] For the structure and dielectric properties studies, both samples were sintered at 1050 °C for 4 h.

Table 1
Surface area, particle size, and chemical compositions of $Bi_{1.5}Zn_{0.92}Nb_{1.5}O_{6.92}$ and $Bi_{1.5}ZnNb_{1.5}O_7$ powders

Type of BZN	Surface area (m^2/g)	Particle size (μm)	Chemical compositions after calcinations (mole)		
			Bi	Zn	Nb
$Bi_{1.5}Zn_{0.92}Nb_{1.5}O_{6.92}$	7.08	0.40	1.42	0.92	1.50
$Bi_{1.5}ZnNb_{1.5}O_7$	7.01	0.43	1.43	1.00	1.50

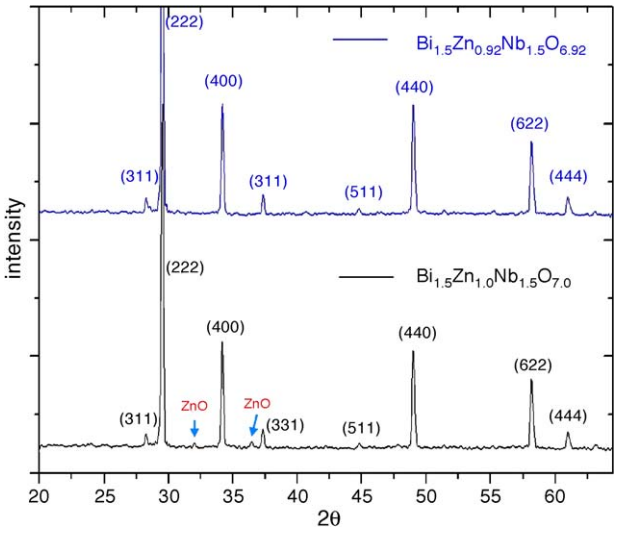

Fig. 1. XRD patterns of $Bi_{1.5}Zn_{0.92}Nb_{1.5}O_{6.92}$ and $Bi_{1.5}ZnNb_{1.5}O_7$.

In order to obtain the distribution of elements in two samples, we used the EPMA technique to map the samples. The metal elements of $Bi_{1.5}Zn_{0.92}Nb_{1.5}O_{6.92}$ are distributed uniformly in the sample as shown in Fig. 2. There is a slight Zn element congregation in the sample of $Bi_{1.5}ZnNb_{1.5}O_7$ as shown in the upper right corner of Fig. 3. Table 2 summaries the results of EPMA–WDS chemical composition analysis of two materials at different locations within the samples. It is interesting to note that in both the samples there are no differences in the grain or at its boundary. Both $Bi_{1.5}Zn_{0.92}Nb_{1.5}O_{6.92}$ and $Bi_{1.5}ZnNb_{1.5}O_7$ crystals exhibit many small voids (<1 μm) which is likely from the loss of volatile Bi during sintering (reduced from 1.43 to 1.42 mol).

In the structure of $Bi_{1.5}Zn_{0.92}Nb_{1.5}O_{6.92}$, 21% of Bi^{+3} atoms are replaced with Zn^{2+} atoms, and 4% of the A position remains vacant (substitutional point defects) that provides room for dielectric relaxation.[10] The temperature dependence of real and imaginary part on the dielectric function for $Bi_{1.5}Zn_{0.92}Nb_{1.5}O_{6.92}$ between 3 MHz and 1.8 GHz is shown in Fig. 4. The dielectric relaxation occurs between 100 and 230 K. The relaxation frequency is shifted to a higher temperature with increasing frequency. Similar behavior was described in Ref.[11] The dielectric relaxation of $Bi_{1.5}Zn_{0.92}Nb_{1.5}O_{6.92}$ at frequencies higher than 1.8 GHz could likely occur at room temperature. The presence of dielectric relaxation will result in high microwave dielectric loss. We have observed a low $Q \times f$ (less than 600) experimentally in the samples at 2.2 GHz (Table 3).

Experimental room temperature infrared reflectivity spectrum of $Bi_{1.5}Zn_{0.92}Nb_{1.5}O_{6.92}$ with its fit is shown in Fig. 5(a). The spectral range above 1000 cm^{-1} is not shown because the reflectivity is flat at frequencies approaching the value given by the high-frequency permittivity ε_∞. The complex dielectric response $\varepsilon^*(\omega)$ in the infrared range can be obtained from the reflectivity $R(\omega)$ spectra via formula[13]:

$$R(\omega) = \left| \frac{\sqrt{\varepsilon^*(\omega)} - 1}{\sqrt{\varepsilon^*(\omega)} + 1} \right|^2 \quad (1)$$

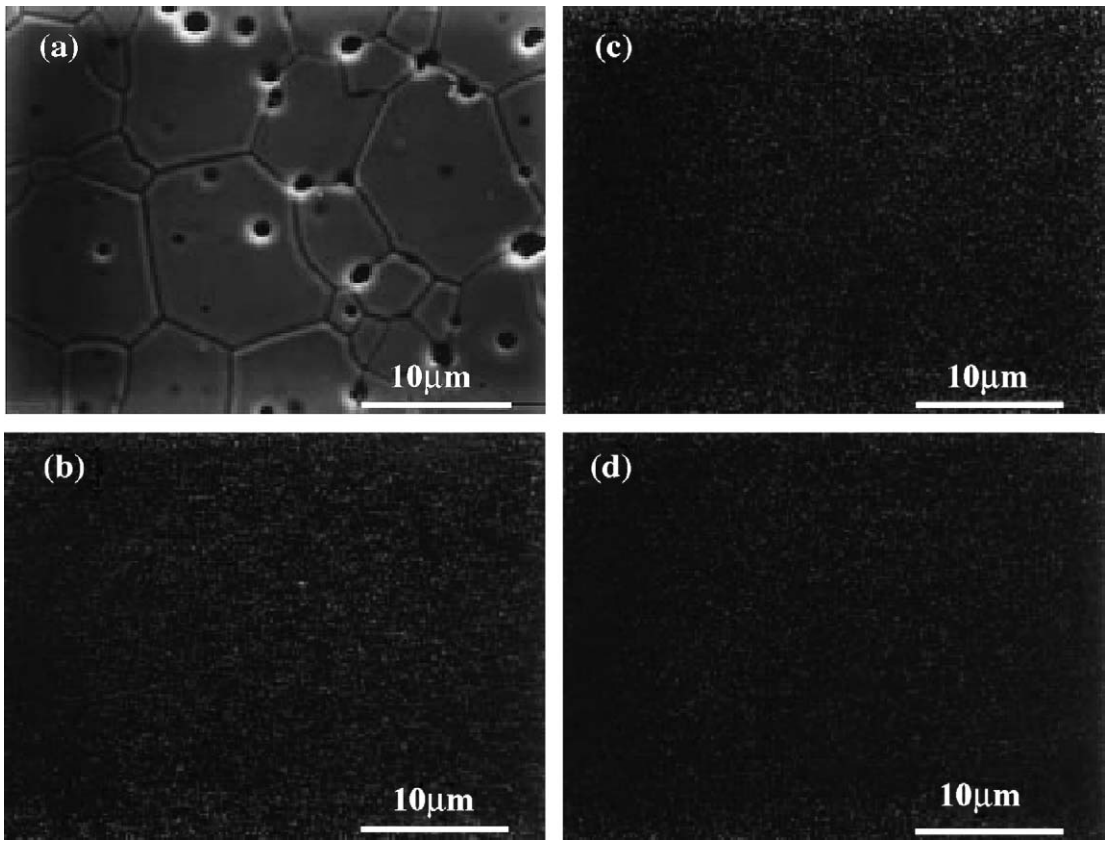

Fig. 2. EPMA element mapping of $Bi_{1.5}Zn_{0.92}Nb_{1.5}O_{6.92}$: (a) microstructure, (b) Bi element mapping, (c) Zn element mapping, and (d) Nb element mapping.

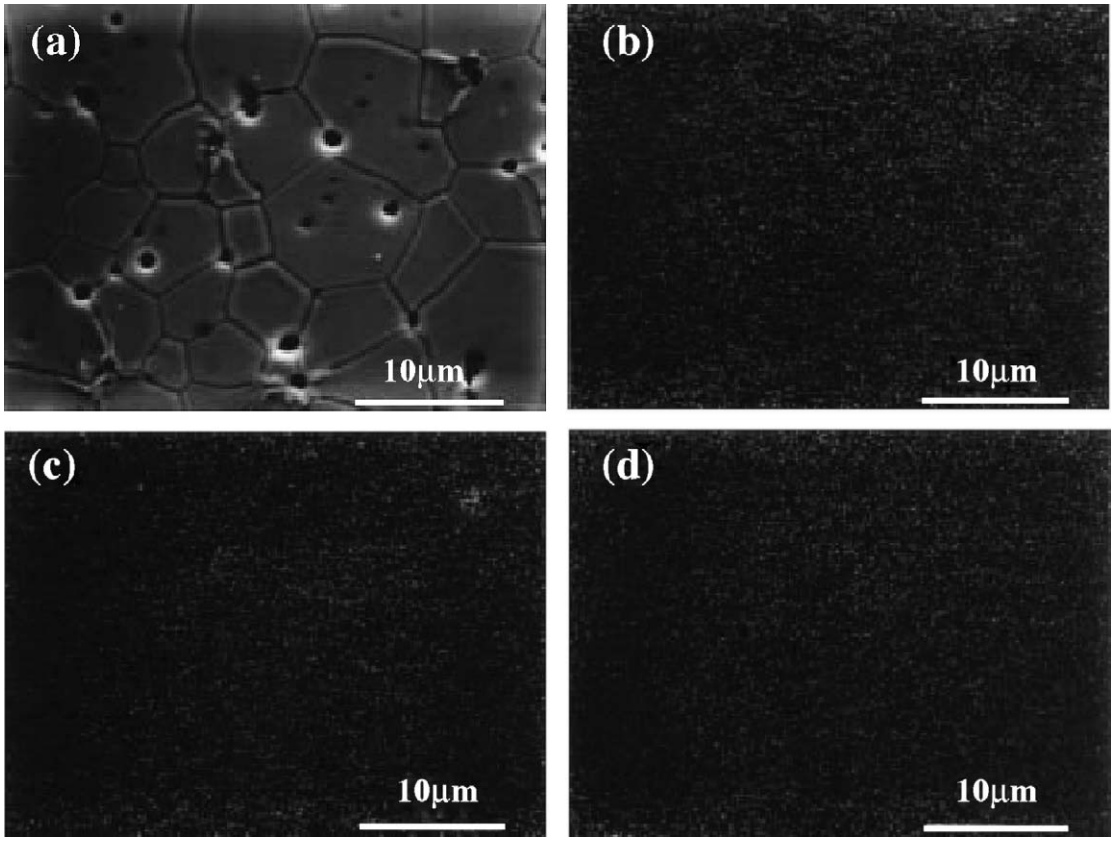

Fig. 3. EPMA element mapping of $Bi_{1.5}ZnNb_{1.5}O_7$: (a) microstructure, (b) Bi element mapping, (c) Zn element mapping, and (d) Nb element mapping.

Table 2
Chemical compositions of sintered $Bi_{1.5}Zn_{0.92}Nb_{1.5}O_{6.92}$ and $Bi_{1.5}ZnNb_{1.5}O_7$ at different locations of the samples

Type of BZN	Locating test at the sample	Chemical compositions after sintering (mole)		
		Bi	Zn	Nb
$Bi_{1.5}Zn_{0.92}Nb_{1.5}O_{6.92}$	In grain	1.43	0.92	1.50
	At grain boundary	1.43	0.92	1.50
$Bi_{1.5}ZnNb_{1.5}O_7$	In grain	1.42	1.00	1.50
	At grain boundary	1.42	1.00	1.50

Table 3
Dielectric properties of $Bi_{1.5}Zn_{0.92}Nb_{1.5}O_{6.92}$ and $Bi_{1.5}ZnNb_{1.5}O_7$ at high frequency

Composition	f (GHz)	ε'	$Q \times f$ (GHz)	Sintering condition
$Bi_{1.5}Zn_{0.92}Nb_{1.5}O_{6.92}$	2.27	121.3	487	1000 °C, 4 h
	2.25	126.2	520	1050 °C, 4 h
	2.22	130.7	368	1100 °C, 4 h
$Bi_{1.5}ZnNb_{1.5}O_7$	2.24	121.2	389	1000 °C, 4 h
	2.24	126.0	426	1050 °C, 4 h
	2.23	130.3	374	1100 °C, 4 h

using the fit procedure of $\varepsilon^*(\omega)$. A generalized oscillator model[13] with the factorized form of the complex dielectric function was used:

$$\varepsilon^*(\omega) = \varepsilon'(\omega) + i\varepsilon''(\omega) = \varepsilon_\infty \prod_{j=1}^{n} \frac{\omega_{LO_j}^2 - \omega^2 + i\omega\gamma_{LO_j}}{\omega_{TO_j}^2 - \omega^2 + i\omega\gamma_{TO_j}} \quad (2)$$

$\omega_{TO_j}^2$ and $\omega_{LO_j}^2$ denote the transverse optical (TO) and longitudinal optical (LO) frequencies of the jth polar mode, respectively, and γ_{TO_j} and γ_{LO_j} are the corresponding damping constants. The ε_∞ denotes high-frequency permittivity originating from electron transitions. The results of the fittings are shown in Fig. 5(a) by dotted lines.

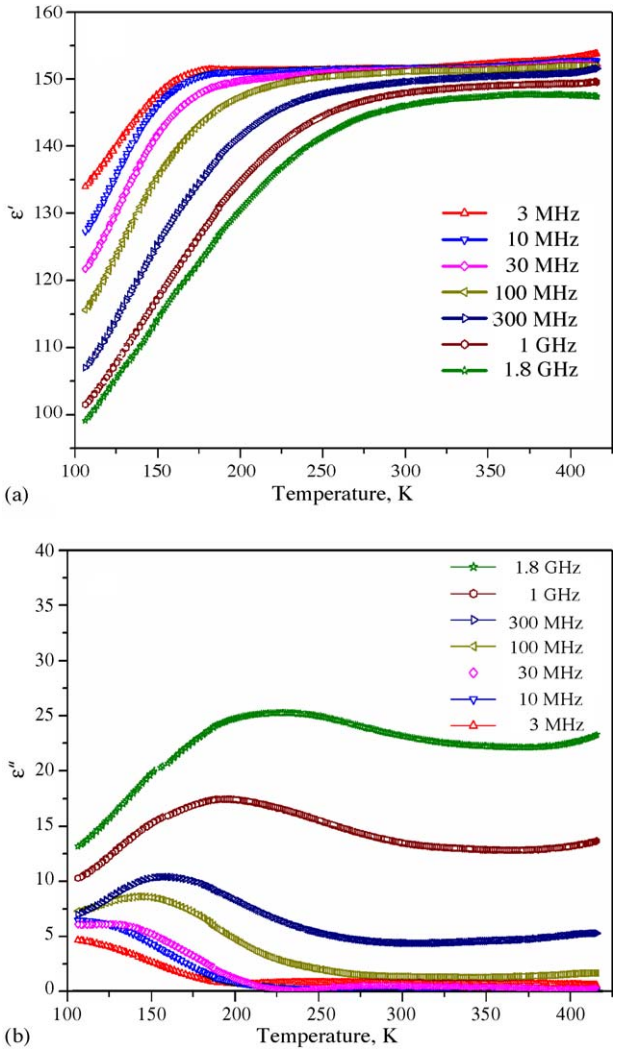

Fig. 4. Temperature dependence of dielectric permittivity at selected frequencies between 3 MHz and 1.8 GHz: (a) real part and (b) imaginary part of dielectric permittivity for $Bi_{1.5}Zn_{0.92}Nb_{1.5}O_{6.92}$.

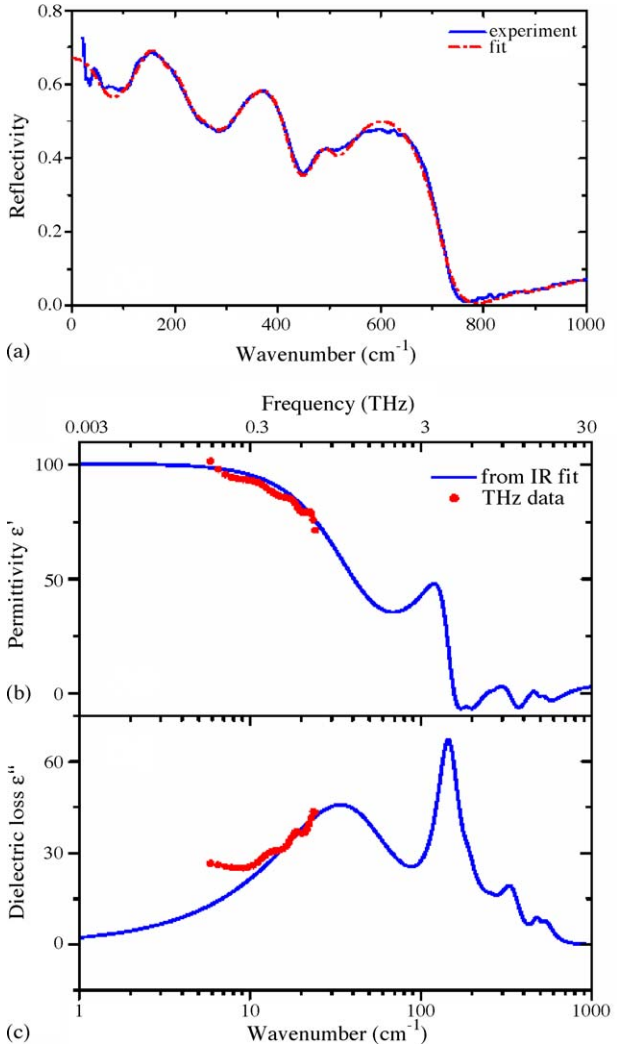

Fig. 5. FTIR and THz spectra of $Bi_{1.5}Zn_{0.92}Nb_{1.5}O_{6.92}$: (a) infrared reflectivities at 300 K, (b) the real part of permittivity, and (c) the imaginary part of permittivity calculated from the fits to the reflectivities and submillimeter data with Eqs. (1) and (2).

The real part ε' (ω) and imaginary part ε'' (ω) of complex permittivity obtained from the fit are shown in Fig. 5(b) and (c) together with experimental THz spectra. The more accurate experimental THz dielectric data were used to fit the infrared reflectivity data of $Bi_{1.5}Zn_{0.92}Nb_{1.5}O_{6.92}$ in the range of 6–30 cm^{-1}. Fig. 5(c) also shows that the oscillator fit is not suitable for description of the THz data below 10 cm^{-1}. The relaxation is probably broader and should be in fact fitted with the distribution of relaxation frequencies and not by overdamped oscillator how it is in our case. The submillimeter permittivity ε' is lower than the permittivity below 2 GHz which gives evidence about the presence of microwave relaxation. This broad relaxation was also seen in $Bi_{1.5}ZnNb_{1.5}O_7$ and fitted in Ref.11 with distribution of relaxations. Levin et al.[12] have shown that the Bi and Zn atoms in the A sites and some O atoms are dynamically disordered among several local potential minima, and Kamba et al.[11] have assigned the relaxation to the local hopping of these disordered atoms. Ref.11 is devoted to $Bi_{1.5}ZnNb_{1.5}O_7$, however, later structural studies of Levin et al.[12] revealed that the sample actually consisted of $Bi_{1.5}Zn_{0.92}Nb_{1.5}O_{6.92}$ and small amounts of ZnO.

We note the broad absorption peak near 30 cm^{-1} in ε'' (ω) spectrum in Fig. 5(c). It was fit to overdamped oscillator and gives evidence about large structural disorder in the BZN lattice. Parameters of the oscillator fit are similar to those already published in Refs.[11,14]. The results indicate that the polar phonon modes are not influenced by small content of ZnO second phase.

The dielectric properties of $Bi_{1.5}Zn_{0.92}Nb_{1.5}O_{6.92}$ and $Bi_{1.5}ZnNb_{1.5}O_7$ at high frequencies are listed in Table 3. Both materials reveal high dielectric constant and low $Q \times f$. Their microwave properties are very similar even when changing the sintering temperatures. However, $Bi_{1.5}Zn_{0.92}Nb_{1.5}O_{6.92}$ exhibits a better $Q \times f$ than that of $Bi_{1.5}ZnNb_{1.5}O_7$ especially for the sample sintered at 1050 °C for 4 h. The excess ZnO in $Bi_{1.5}ZnNb_{1.5}O_7$ may produce interstitial defects appearing in the cubic pyrochlore crystalline structure. Such defects would reduce the $Q \times f$ of $Bi_{1.5}ZnNb_{1.5}O_7$.

4. Conclusions

Ceramics of $Bi_{1.5}ZnNb_{1.5}O_7$ and $Bi_{1.5}Zn_{0.92}Nb_{1.5}O_{6.92}$ were successfully prepared. Our microstructure study of $Bi_{1.5}ZnNb_{1.5}O_7$ shows that it consists of cubic pyrochlore structure of $Bi_{1.5}Zn_{0.92}Nb_{1.5}O_{6.92}$ and small amounts of ZnO. For pure $Bi_{1.5}Zn_{0.92}Nb_{1.5}O_{6.92}$, a broad dielectric relaxation that peaks around 230 K was observed at 1.8 GHz, which is similar to the relaxation of $Bi_{1.5}ZnNb_{1.5}O_7$ seen in Ref.11. Nevertheless, the $Bi_{1.5}Zn_{0.92}Nb_{1.5}O_{6.92}$ has systematically slightly higher $Q \times f$ than that of $Bi_{1.5}ZnNb_{1.5}O_7$. It is probably due to interstitial defects from ZnO second phase presented in $Bi_{1.5}ZnNb_{1.5}O_7$. Highly disordered pyrochlore structure results not only in broad microwave dielectric relaxation but also in broad excitation in submillimetre range, which is probably activated phonon density of states in FTIR and THz spectra. Both $Bi_{1.5}ZnNb_{1.5}O_7$ and $Bi_{1.5}Zn_{0.92}Nb_{1.5}O_{6.92}$ reveal high dielectric constant (>120) and low $Q \times f$ (<600) at 2.2 GHz. The low $Q \times f$ results from the dielectric relaxation and voids present in the samples.

Acknowledgments

Financial support obtained from the National Science Council of Republic of China (NSC91-2622-E-007-032, NSC92-2120-E-002-002, and NSC93-2120-M-002-010), and Academy of Sciences of the Czech Republic (A1010213) is highly appreciated. We are grateful to An-Jey Su of University of Pittsburgh for editing this manuscript and to A. Pashkin for doing the THz spectra measurements.

References

1. Wu, Z. M., *The Study of Low Sintering BZN Microwave Ceramics by Adding V2O5*. M.S. thesis of National Chin-Hwa University, Taiwan, 1999.
2. Ling, H. C., Yan, M. F. and Rhodes, W. W., High dielectric constant and small temperature coefficient bismuth-based dielectric compositions. *J. Mater. Res.*, 1990, **5**(8), 1752–1762.
3. Yan, M. F., Ling, H. C. and Rhodes, W. W., Low-firing, temperature-stable dielectric compositions based on bismuth nickel zinc niobates. *J. Am. Ceram. Soc.*, 1990, **73**, 1106–1107.
4. Liu, D., Liu, Y., Huang, S. and Yao, X., Phase structure and dielectric properties of Bi_2O_3-ZnO-Nb_2O_5-based dielectric ceramics. *J. Am. Ceram. Soc.*, 1993, **76**(8), 2129–2132.
5. Hu, Y. and Huang, C. L., Structure and dielectric properties of bismuth-based dielectric ceramics. *Mater. Chem. Phys.*, 2001, **72**, 60–65.
6. Yee, K. A. and Han, K. R., The effect of V_2O_5 on the sinterability and physical properties of Bi_2O_3-NiO-Nb_2O_5 and Bi_2O_3-ZnO-Nb_2O_5 temperature-stable dielectrics. *J. Mater. Sci.*, 1999, **34**, 4699–4704.
7. Cann, D. P., Randall, C. A. and Shrout, T. R., Investigation of the dielectric properties of bismuth pyrochlores. *Solid State Commun.*, 1996, **100**(7), 529–534.
8. Wu, M. C., *Study on Zn–Nb series low sintering temperature microwave dielectric material for applications in wireless communication*. Master thesis, July 2004.
9. Su, W. F. and Lin, S. C., Interfacial behaviour between $Bi_{1.5}ZnNb_{1.5}O_7$.0.02V_2O_5 and Ag. *J. Eur. Ceram. Soc.*, 2003, **23**, 2593–2596.
10. Nino, J. C., Lanagan, M. T. and Randall, C. A., Dielectric relaxation in Bi_2O_3-ZnO-Nb_2O_5 cubic pyrochlore. *J. Appl. Phys.*, 2001, **89**(8), 4512–4516.
11. Kamba, S., Porokhonskyy, V., Pashkin, A., Bovtun, V., Petzelt, J., Nino, J. C. *et al.*, Anomalous broad dielectric relaxation in $Bi_{1.5}ZnNb_{1.5}O_7$ pyrochlore. *Phys. Rev. B*, 2002, **66**. pp. 054106/1–8.
12. Levin, I., Amos, T. G., Nino, J. C., Vanderah, T. A., Randall, C. A. and Lanagan, M. T., Structural study of an unusual cubic pyrochlore $Bi_{1.5}Zn_{0.92}$ $Nb_{1.5}O_{6.92}$. *J. Solid State Chem.*, 2002, **168**, 69–75.
13. Petzelt, J. and Kamba, S., Submillimetre and infrared response of microwave materials: extrapolation to microwave properties. *Mater. Chem. Phys.*, 2003, **79**, 175–180.
14. Nino, J. C., Lanagan, M. T., Randall, C. A. and Kamba, S., Correlation between infrared phonon modes and dielectric relaxation in Bi_2O_3-ZnO-Nb_2O_5 cubic pyrochlore. *Appl. Phys. Lett.*, 2002, **81**, 4404–4406.